



Contents lists available at ScienceDirect

Journal of Great Lakes Research

journal homepage: www.elsevier.com/locate/jglr

Anaerobic methane oxidation and aerobic methane production in an east African great lake (Lake Kivu)

Fleur A.E. Roland^{a,*}, Cédric Morana^b, François Darchambeau^a, Sean A. Crowe^c, Bo Thamdrup^d, Jean-Pierre Descy^{a,e}, Alberto V. Borges^a

^a Chemical Oceanography Unit, Université de Liège, Belgium

^b Department of Earth and Environmental Sciences, Katholieke Universiteit Leuven (KU Leuven), Belgium

^c Departments of Microbiology and Immunology and Earth, Ocean and Atmospheric Sciences, University of British Columbia, Canada

^d Institute of Biology and Nordic Center for Earth Evolution, University of Southern Denmark, Denmark

^e Laboratory of Freshwater Ecology, URBE, Department of Biology, UNamur, Belgium

ARTICLE INFO

Article history:

Received 23 January 2017

Received in revised form 5 March 2018

Accepted 8 March 2018

Available online xxxx

Associate Editor: Robert E. Hecky

Keywords:

Anaerobic methane oxidation

Tropical lake

Lake Kivu

Aerobic methane production

ABSTRACT

We investigated CH₄ oxidation in the water column of Lake Kivu, a deep meromictic tropical lake with CH₄-rich anoxic deep waters. Depth profiles of dissolved gases (CH₄ and N₂O) and a diversity of potential electron acceptors for anaerobic CH₄ oxidation (NO₃⁻, SO₄²⁻, Fe and Mn oxides) were determined during six field campaigns between June 2011 and August 2014. Denitrification measurements based on stable isotope labelling experiments were performed twice. In addition, we quantified aerobic and anaerobic CH₄ oxidation, NO₃⁻ and SO₄²⁻ consumption rates, with and without the presence of an inhibitor of SO₄²⁻-reducing bacteria activity. Aerobic CH₄ production was also measured in parallel incubations with the addition of an inhibitor of aerobic CH₄ oxidation. The maximum aerobic and anaerobic CH₄ oxidation rates were estimated to be 27 ± 2 and 16 ± 8 μmol/L/d, respectively. We observed a difference in the relative importance of aerobic and anaerobic CH₄ oxidation during the rainy and the dry season, with a greater role for aerobic oxidation during the dry season. Lower anaerobic CH₄ oxidation rates were measured in presence of molybdate in half of the measurements, suggesting the occurrence of linkage between SO₄²⁻ reduction and anaerobic CH₄ oxidation. NO₃⁻ consumption and dissolved Mn production rates were never high enough to sustain the measured anaerobic CH₄ oxidation, reinforcing the idea of a coupling between SO₄²⁻ reduction and CH₄ oxidation in the anoxic waters of Lake Kivu. Finally, significant rates (up to 0.37 μmol/L/d) of pelagic CH₄ production were also measured in oxygenated waters.

© 2018 International Association for Great Lakes Research. Published by Elsevier B.V. All rights reserved.

Introduction

Due to methane's (CH₄) potential impact in global warming and its increase due to human activities, its biogeochemical cycle, including the microbial metabolisms, methanogenesis and methanotrophy, have been widely studied across a broad variety of environments. Global CH₄ emissions have recently been estimated at 553 Tg CH₄/yr for the period 2000–2009, of which 64% is emitted from the tropics (Kirschke et al., 2013; Saunio et al., 2016). Decadal variations in the annual atmospheric CH₄ growth rate have also been attributed to changes in emissions from tropical wetlands (Nisbet et al., 2016). Previous studies estimated that 9.5% of CH₄ is released to the atmosphere from tropical freshwaters and the rest from non-tropical freshwaters (14%), marine ecosystems (3%), human activities (63%), plants (6%), gaseous hydrates (2%) and termites (3%) (Conrad, 2009; Bastviken et al., 2011). The gross CH₄ production rate in these systems is higher, but a large percentage is

biologically oxidized (aerobically or anaerobically) before reaching the atmosphere (Bastviken et al., 2002). Anaerobic CH₄ oxidation (AOM) has been widely observed in marine environments where it is mainly coupled to sulfate (SO₄²⁻) reduction (e.g. Iversen and Jørgensen, 1985; Boetius et al., 2000; Jørgensen et al., 2001). Comparatively, in situ AOM has been less frequently measured in freshwaters environments (e.g. in Lake Rotsee; Schubert et al., 2010), and is often considered as negligible compared to aerobic CH₄ oxidation due to lower SO₄²⁻ concentrations than in seawater (Rudd et al., 1974). However, other potential electron acceptors for AOM, such as nitrate (NO₃⁻), iron (Fe) and manganese (Mn) oxides (Borrel et al., 2011; Cui et al., 2015), can be found in non-negligible concentrations in freshwater environments. AOM coupled to NO₃⁻ reduction (NDMO) has been observed in laboratory or enrichment experiments (e.g. Raghoebarsing et al., 2006; Ettwig et al., 2010; Hu et al., 2011; Haroon et al., 2013; á Nordi and Thamdrup, 2014), but its natural significance remains poorly known. Numerous studies identified the presence of prokaryotes thought capable of NDMO in diverse environments (e.g. Lake Constance, paddy soils, sediments of rivers, etc.; Deutzmann and Schink, 2011; Wang et al.,

* Corresponding author.

E-mail address: froland@uliege.be (F.A.E. Roland).

2012; Shen et al., 2014); but to our knowledge, only one study reports the natural occurrence of this process in soils of Chinese wetlands (Hu et al., 2014). Also, AOM coupled to the reduction of Fe and Mn oxides has been reported from some freshwater environments (e.g. in lakes Matano and Kinneret; Crowe et al., 2011; Sivan et al., 2011; á Norði et al., 2013) and marine sediments (Beal et al., 2009), and Fe-driven AOM has been recently demonstrated in enrichment cultures (Ettwig et al., 2016). But to our best knowledge, no in situ measurements have been reported.

It is generally assumed that CH₄ is almost exclusively produced anaerobically by methanogenic archaea (Borrel et al., 2011). However, growing evidences suggest that CH₄ can also be produced under aerobic conditions in freshwaters (Grossart et al., 2011; Bogard et al., 2014; Tang et al., 2014, 2016) and marine environments (Karl et al., 2008; Lenhart et al., 2016). Different mechanisms of CH₄ production have been hypothesized: demethylation of organic compounds produced by phytoplankton (e.g. dimethylsulfoniopropionate (DMSP), methylphosphonate), hydrogenotrophic or acetoclastic CH₄ production in anoxic microsites or aerobic CH₄ production by oxygen tolerant methanogenic archaea (Jarrell, 1985; Angel et al., 2011; Grossart et al., 2011). Alternatively, CH₄ may be released directly by phytoplankton cells (Lenhart et al., 2016).

Lake Kivu is a deep (maximum depth: 485 m) meromictic lake characterized by large quantities of CH₄ (60 km³ at 0 °C and 1 atm) dissolved in its deep anoxic waters, yet it is a minor emitter of CH₄ to the atmosphere due to intense CH₄ oxidation (Borges et al., 2011; Roland et al., 2016). To date, CH₄ oxidation in Lake Kivu was measured by Jannasch (1975) on a single station at four depths, and was estimated from mass balance (Pasche et al., 2011) and stable isotope composition change (Morana et al., 2015a). Indirect evidence of AOM coupled to SO₄^{2−} reduction in Lake Kivu comes from microbial community composition (Inceoglu et al., 2015; Zigah et al., 2015) that showed the co-occurrence of sulfate-reducing and methanotrophic micro-organisms. Isotopic analyses (Morana et al., 2015a) revealed the occurrence of both aerobic and anaerobic CH₄ oxidation in the water column of Lake Kivu, and suggested that aerobic CH₄ oxidation was probably the main pathway of CH₄ removal. None of these studies, however, directly demonstrated and quantified aerobic and anaerobic oxidation rates while little was known about seasonal and spatial variability in CH₄ oxidation within Lake Kivu and the diversity of potential electron acceptors involved in AOM. Given that SO₄^{2−} concentrations are moderate (100–200 μmol/L; Pasche et al., 2009; Morana et al., 2016) and that NO₃[−] accumulates at the oxic-anoxic interface during the rainy season (Roland et al., 2016), we hypothesized that AOM could be uniquely driven through SO₄^{2−} reduction during the dry season, while AOM coupled to both NO₃[−] and SO₄^{2−} reduction (NDMO and SDMO, respectively) would together support AOM during the rainy season. We also evaluated the potential for Fe and Mn oxide-dependent AOM and, to fully quantify the CH₄ cycle in the water column, we also determined rates of aerobic CH₄ production in the oxic mixed layer.

Material and methods

Sampling sites

Lake Kivu is an East African great lake located at the border between Rwanda and the Democratic Republic of the Congo (Fig. 1). It is divided into one main basin, two small basins and two bays: Northern Basin (or main basin), Southern Basin (or Ishungu Basin), Western Basin (or Kalehe Basin), the bay of Kabuno in the north and the bay of Bukavu in the South. Six field campaigns were conducted in the main basin (the Northern Basin off Gisenyi; −1.72504°N, 29.23745°E) in June 2011 (early dry season), February 2012 (rainy season), October 2012 (late dry season), May 2013 (late rainy season), September 2013 (dry season) and August 2014 (dry season).

Physico-chemical parameters and sampling

Vertical profiles of temperature, conductivity, pH and oxygen were obtained with a Yellow Springs Instrument 6600 V2 multiparameter probe. Sensors characteristics are detailed in ESM Table S1. Water was collected with a 7 L Niskin bottle (Hydro-Bios) every 2.5 m in a ~10 m zone centered on the oxic-anoxic interface.

Chemical analyses

Samples for CH₄ and N₂O concentrations were collected in 60 ml glass serum bottles, filled directly from the Niskin bottle with tubing, left to overflow, poisoned with 200 μl of saturated HgCl₂ solution, and sealed with grey butyl stoppers (Wheaton, USA) and aluminum crimp caps. The butyl stoppers were previously boiled in milli-Q water in the laboratory. CH₄ and N₂O concentrations were determined via the headspace equilibration technique (20 ml N₂ headspace in 50 ml serum bottles, for samples of the main basin) and measured by gas chromatography (GC) (Weiss, 1981) with electron capture detection (ECD) for N₂O and with flame ionization detection (FID) for CH₄, as described by Borges et al. (2015). The SRI 8610C GC-ECD-FID was calibrated with certified CH₄:CO₂:N₂O:N₂ mixtures (Air Liquide, Belgium) of 1, 10, 30 and 509 ppm CH₄ and of 0.2, 2.0 and 6.0 ppm N₂O. Concentrations were computed using the solubility coefficients of Yamamoto et al. (1976) and Weiss and Price (1980), for CH₄ and N₂O, respectively. The precision of measurements was ±3.9% and ±3.2% for CH₄ and N₂O, respectively.

Samples for nutrients analyses were collected in 50 ml plastic vials after being filtered through a 0.22 μm syringe filter. Then, 200 μl of 5 N H₂SO₄ were added to each vial for preservation. Samples were then frozen. NO₂[−] concentrations were determined by the sulfanilamide method (APHA, 1998), using a 5-cm light path on a Thermo Spectronic Genesys 10vis spectrophotometer. NO₃[−] concentrations were determined after vanadium reduction to NO₂[−] and quantified under this form by spectrophotometry with a Multiskan Ascent Thermo Scientific multi-well plate reader (APHA, 1998; Miranda et al., 2001). The detection limits for these methods were 0.03 and 0.15 μmol/L for NO₂[−] and NO₃[−], respectively.

Samples for sulfide (HS[−]) concentrations were collected in 50 ml plastic vials, after being filtered through a 0.22 μm syringe filter. Samples were preserved with 200 μl of 20% zinc acetate (ZnAc) and were stored frozen. HS[−] concentrations were quantified using a 5-cm light path on a spectrophotometer, according to the method described by Cline (1969). Samples for SO₄^{2−} analyses were filtered through a 0.22 μm syringe filter and collected in 5 ml Cryotube vials. Samples were preserved with 20 μl of 20% ZnAc and were stored frozen. SO₄^{2−} concentrations were determined by ion chromatography (Dionex ICS-1500, with an autosampler Dionex AS50, a guard column Dionex AG22 and an analytical column Dionex IonPac AS22). The detection limits of these methods were 0.25 and 0.5 μmol/L for HS[−] and SO₄^{2−}, respectively.

In May 2013, September 2013 and August 2014, samples for Fe and Mn measurements were collected into 50 ml-plastic syringes directly from the Niskin bottle. Water was rapidly transferred from the syringe to the filtration set and was passed through 25 mm glass fiber filters (0.7 μm pore size). Filters were collected in 2 ml Eppendorf vials and preserved with 1 ml of a HNO₃ 2% solution while filtrates were collected into four 2 ml Eppendorf vials and preserved with 20 μl of a HNO₃ 65% solution. The filters, for particulate Fe and Mn determination, were digested with nitric acid in Teflon bombs in a microwave digestion apparatus (Ethos D, Milestone Inc.). They were finally diluted with milli-Q water to a volume of 50 ml. Filtrates were directly diluted with milli-Q water to a volume of 50 ml. Fe and Mn concentrations were determined by inductively coupled plasma mass spectrometry (ICP-MS) using dynamic reaction cell (DRC) technology (ICP-MS SCIEX ELAN DRC II, PerkinElmer Inc.). Analytical accuracy was verified by a certified reference material (BCR 715, Industrial Effluent Wastewater).

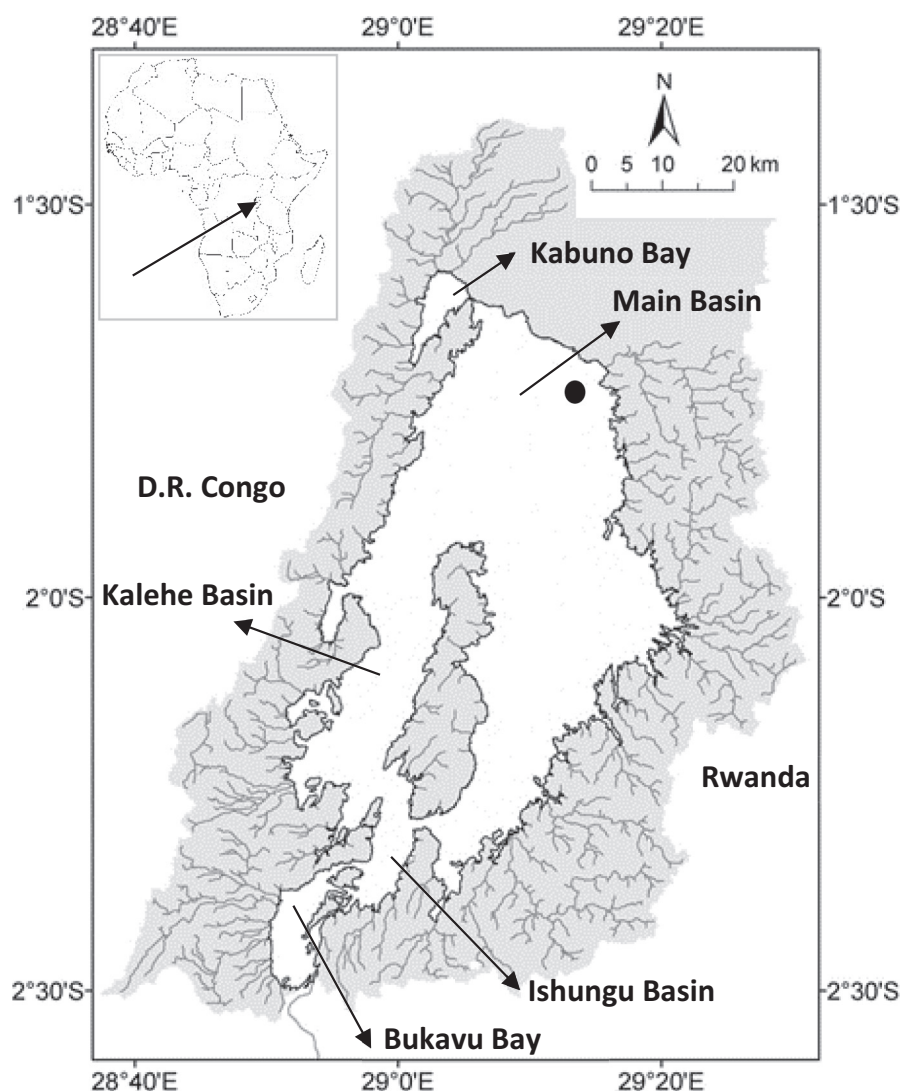


Fig. 1. Map of Lake Kivu, showing the different basins and bays, and the sampling site in the main basin (black dot).

CH₄ oxidation, NO₃⁻ and SO₄²⁻ consumption and Mn²⁺ production rates measurements

Samples for CH₄ oxidation rate measurements were collected in 60 ml serum bottles according to the method described above. At each depth, two bottles were directly poisoned with 200 µl of HgCl₂ injected through the septum with a syringe. Ten other bottles were incubated in the dark and at constant temperature close to the in situ temperature of ~23 °C. Five serum bottles received 250 µl of a solution of sodium molybdate (final concentration of 4 mmol/L), an inhibitor of sulfate-reducing bacteria activity (Yadav and Archer, 1989); and five received no molybdate amendment. At each of the 5 time steps (12 h, 24 h, 48 h, 72 h, 96 h), the microbial activity was stopped in one amended and one non-amended bottle with the addition of 200 µl of a saturated solution of HgCl₂.

In all the incubated bottles, CH₄ and NO₃⁻ concentrations were determined as described above. In addition to these measurements, Mn, Fe and SO₄²⁻ concentrations were determined in August 2014. Mn and Fe concentrations were quantified following the method described above while SO₄²⁻ concentrations were measured by spectrophotometry using a 5-cm light path on a spectrophotometer Thermo Spectronic Genesys 10vis, following the nephelometric method described by Rodier et al. (1996), after precipitation of barium sulfate in an acid environment. The detection limit of this method was 52 µmol/L.

CH₄ oxidation, NO₃⁻ and SO₄²⁻ consumption and Mn²⁺ and Fe²⁺ production rates were calculated as linear regressions of CH₄, NO₃⁻, SO₄²⁻ and Mn²⁺ and Fe²⁺ concentrations as a function of time over the course of the incubation. ESM Table S2 shows initial CH₄ concentrations, percentage of CH₄ consumed and the time lapses during which the CH₄ oxidation rates were calculated for each depth. Potential AOM rates were also calculated based on the NO₃⁻ consumption, denitrification and SO₄²⁻ consumption rates measured in the incubations, following the stoichiometry of each equation (ESM Table S3).

It cannot be excluded that a small amount of O₂ was introduced at the start of the incubation in the bottles amended with molybdate. Therefore, CH₄ oxidation rates measured with molybdate were corrected by taking into account the oxygen potentially supplied with the addition of the molybdate solution. As the O₂ concentrations of the molybdate solution were likely at saturation with respect to air, we considered here that 1.25 µmol/L of O₂ was added to each bottle (250 µl of the solution was added to 60 ml of lake water). The O₂ concentration required for a given rate of CH₄ oxidation was calculated according to the stoichiometric Eq. A in ESM Table S3.

The fraction of CH₄ oxidation potentially due to O₂ was then calculated according to Eq. (1):

$$Ro = Rm^* (O_{2r}/O_{2a}) \quad (1)$$

where R_o is the fraction of oxidation due to O_2 (supplied with the molybdate solution), R_m is the measured oxidation rate, O_{2r} is the O_2 concentration required for the measured CH_4 oxidation rate and O_{2a} is the O_2 concentration added with the molybdate solution.

The corrected CH_4 oxidation rates with molybdate were obtained by subtraction (Eq. 2):

$$\text{Corrected } CH_4 \text{ oxidation rate with Mo} = R_m - R_o \quad (2)$$

All rates with molybdate reported here are corrected CH_4 oxidation rates.

Pelagic CH_4 production rate measurements

In May 2013, September 2013 and August 2014, samples for pelagic CH_4 production measurements were collected in 60 ml glass serum bottles, according to the method described above. At each depth, two bottles were directly poisoned with 200 μ l of $HgCl_2$ injected through the septum with a syringe while 5 bottles received 500 μ l of a solution of picolinic acid (final concentration of 0.1 mmol/L), an inhibitor of aerobic CH_4 oxidation (Megraw and Knowles, 1990). Bottles were incubated in the dark and at constant temperature close to the in situ temperature of $\sim 23^\circ C$. The microbial activity in these bottles was stopped with the addition of 200 μ l of a saturated $HgCl_2$ after 12 h, 24 h, 48 h, 72 h, and 96 h. Measurement of the CH_4 concentrations in every incubated bottle was performed following the procedure described above. CH_4 production rates were calculated as the linear increase of the CH_4 concentrations during the incubation.

Vertical fluxes calculations

The vertical fluxes (F_{vertical}) of SO_4^{2-} , Mn^{2+} , and Fe^{2+} were calculated as described by Pasche et al. (2009) (Eq. 3):

$$F_{\text{vertical}} = -D_{\text{turbulent}} \cdot \text{Grad} + C \cdot \text{Adv} \quad (3)$$

where $D_{\text{turbulent}}$ is the turbulent diffusion coefficient, Grad is the vertical concentration gradient of each element, C is the concentration of the element at a given depth, and Adv is the upwelling velocity.

A turbulent diffusion coefficient of 0.000001 m^2/s and an upwelling velocity of 0.00000022 m/s were used for the calculations, as determined by Pasche et al. (2009).

N stable isotope labelling experiments

In May and September 2013, parallel denitrification experiments were conducted in order to link this process with CH_4 oxidation. Water was collected with the Niskin bottle, transferred with tubing to two amber 250 ml borosilicate bottles which were left to overflow and sealed with Polytetrafluoroethylene coated screw caps. Before the injection of ^{15}N -labeled solutions, a 12 h pre-incubation period in the dark and at $25^\circ C$ was observed in order to allow the consumption of oxygen inadvertently introduced to the bottles during sampling.

N stable isotope labelling experiments were based on Thamdrup and Dalsgaard (2002). Heterotrophic denitrification was determined by the injection of a $Na^{15}NO_3$ solution to the amber bottles, through the stopper (final concentration of 5 μ mol/L). Six 12 ml vials (Labco Exetainer) were then filled from each of the duplicate bottles and placed in a dark incubator at ambient temperature ($24^\circ C$), which was close to the in situ temperature ($\sim 23^\circ C$). Microbial activity in two Exetainers was immediately arrested through the addition of 500 μ l 20% ZnAc. A time course was established by arresting two further Exetainers at 6, 12, 18, 24 and 48 h. While injecting ZnAc solution to stop the incubations of the Exetainers, the excess water was collected in 2 ml-Eppendorf vials and stored frozen to determine the change of the NO_3^- concentrations through time. NO_3^- were then analyzed by

chemiluminescence, after reduction with vanadium chloride (VCl_3), with an NO_2^- , NO_3^- and NO_x analyzer (Thermo Environmental Instruments), according to the method described by Braman and Hendrix (1989) (detection limit: 2–3 ng NO_x).

$^{29}N_2$ and $^{30}N_2$ concentrations in the Exetainers were measured with a gas source isotope ratio mass spectrometer (Delta V Plus, ThermoScientific) after creating a 2 ml helium headspace (volume injected in the mass spectrometer: 50 μ l). Potential denitrification rates (detection limits of 2.7 nmol/L/h) in the incubations with $^{15}NO_3^-$ were calculated according to Eq. (4) (Thamdrup and Dalsgaard, 2002):

$$\text{Potential } N_2 \text{ denitrification} = ^{15}N^{15}N_{\text{excess}} * (F_{NO_3})^{-2} \quad (4)$$

where $N_2 \text{ denitrification}$ is the production of N_2 by denitrification during the incubations with $^{15}NO_3^-$. $^{15}N^{15}N_{\text{excess}}$ is the production of excess $^{15}N^{15}N$ and F_{NO_3} is the fraction of $^{15}NO_3^-$ added in the NO_x pool. NO_x concentrations of the NO_x pool were measured in the incubations as described above. $^{15}N^{15}N$ is the excess relative to the mass 30: mass 28 ratio in the time zero gas samples.

Denitrification rates were calculated from potential denitrification rates, according to Eq. (5) (Roland et al., 2017):

$$N_2 \text{ denitrification} = \text{Potential } N_2 \text{ denitrification} * (1 - F_{NO_3}) \quad (5)$$

which assumes that the rate follows first order kinetics with respect to NO_3^- .

Pigment analysis

In May 2013, September 2013 and August 2014, samples for pigments analyses were collected on Whatman GF/F 47 mm glass fiber filters (filtration volumes: 3 L). Filters were preserved in 5 ml Cryotube vials and stored frozen until pigment extraction in 4 ml of 90% HPLC grade acetone. Two 15-min sonications separated by an overnight period at $4^\circ C$ in dark were applied, and extracts were stored in 2 ml-amber borosilicate vials. HPLC analyses were carried out as described by Sarmiento et al. (2006).

Results

Physical and chemical characteristics of the water column

Vertical profiles of physico-chemical variables differed strongly between stations and campaigns (Fig. 2). In the dry season, the water column was anoxic below 47.5, 57.5, 55 and 60 m in June 2011, October 2012, September 2013 and August 2014, respectively. During the rainy season, it was anoxic below 45 and 55 m in February 2012 and May 2013, respectively. At each date, the thermocline and chemocline (based on specific conductivity and pH, respectively) mirrored the oxycline and temperature at the oxic-anoxic interface averaged $23.5 \pm 0.2^\circ C$ (mean \pm standard deviation).

CH_4 concentrations were low ($0.3 \pm 0.5 \mu$ mol/L) from the surface to 45–55 m where they started to increase; at 70 m, CH_4 concentrations were $385 \pm 43 \mu$ mol/L (Fig. 3). For all campaigns, N_2O concentrations were higher in oxic waters (7.0 ± 0.4 nmol/L from 0 to 40 m) than in anoxic waters (1.3 ± 0.8 nmol/L below 60 m depth). In February 2012 and September 2013, peaks of N_2O up to 15 nmol/L were observed at 50 m (anoxic waters) and at 45 m (oxic waters), respectively.

NO_x profiles also reflected the seasonal variations of the water column characteristics. No zones of NO_x accumulation (nitracline) were observed in June 2011 and May 2013, and a weak NO_x maxima ($<2 \mu$ mol/L at 52.5 m) was observed in August 2014. In February 2012, October 2012 and September 2013, NO_x maxima of 3 μ mol/L (at 50 m), 4 μ mol/L (at 50 m) and 4 μ mol/L (at 47.5 m), respectively, were observed. The mean vertical upward flux of NH_4^+ was 0.42 ± 0.19 mmol/ m^2/d . SO_4^{2-} and H_2S concentrations did not show strong variation between

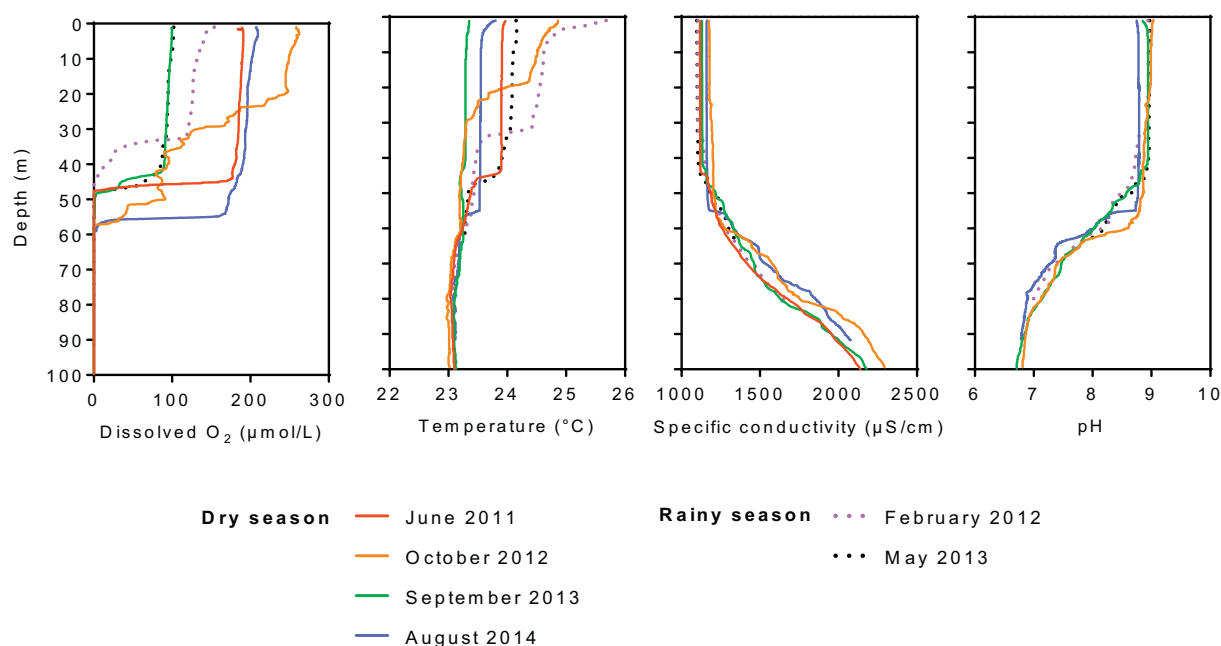


Fig. 2. Vertical profiles of dissolved oxygen ($\mu\text{mol/L}$), temperature ($^{\circ}\text{C}$), specific conductivity ($\mu\text{S/cm}$) and pH for the six field campaigns.

the different campaigns. The mean of SO_4^{2-} concentrations in oxic waters (from 0 to 50 m depth) was $153 \pm 21 \mu\text{mol/L}$, while the mean of H_2S concentrations in anoxic waters (at 70 m depth) was $42 \pm 25 \mu\text{mol/L}$. SO_4^{2-} concentrations strongly decreased in the anoxic zone (to $<0.5 \mu\text{mol/L}$ at 80 m depth) while HS^- concentrations increased with increasing depth. The mean vertical downward flux of SO_4^{2-} was $0.30 \pm 0.09 \text{ mmol/m}^2/\text{d}$.

While particulate Fe concentrations were up to $15 \mu\text{mol/L}$ in oxic waters, in September 2013, dissolved Fe concentrations were very low ($<2.5 \mu\text{mol/L}$ all along the vertical profiles, during the three field campaigns). On the contrary, particulate Mn concentrations were low ($<2 \mu\text{mol/L}$), with a maximum concentration peak located just above the oxic-anoxic interface, for the three campaigns, and dissolved Mn concentrations increased with depth to maximum concentrations of 10

$\mu\text{mol/L}$ in anoxic waters. The mean vertical upward fluxes of Fe^{2+} and Mn^{2+} were $0.003 \pm 0.001 \text{ mmol/m}^2/\text{d}$ and $0.033 \pm 0.006 \text{ mmol/m}^2/\text{d}$, respectively.

Microbial process rate measurements

CH_4 oxidation was detected during all field campaigns (Fig. 4). The dry season was characterized by higher maximum CH_4 oxidation rates in oxic waters than anoxic waters. The maximal oxic and anoxic oxidation rates were observed in August 2014, and were 27 ± 2 (at 55 m) and 16 ± 8 (at 75 m) $\mu\text{mol/L/d}$, respectively. A correspondingly high SO_4^{2-} consumption rate of $7.5 \pm 0.0 \mu\text{mol/L/d}$ (ESM Table S4) was observed within the vicinity of this high CH_4 oxidation rate, at 70 m depth. During the other field campaigns, maximum oxic CH_4 oxidation

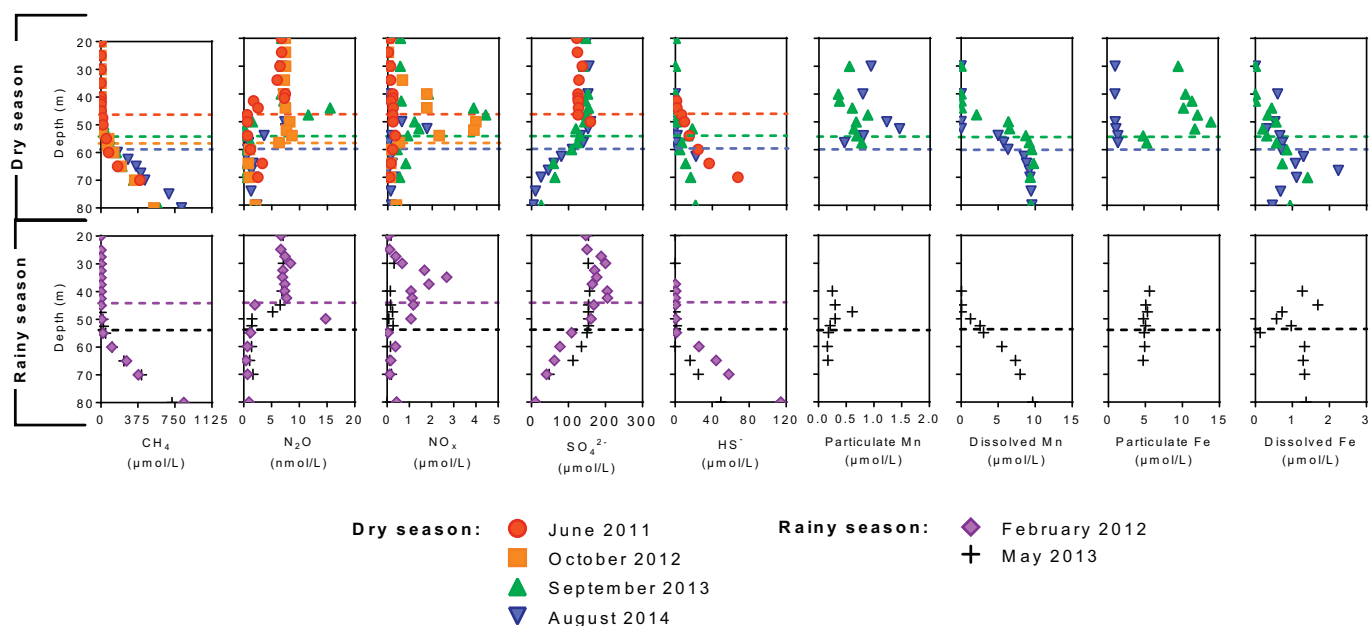


Fig. 3. Vertical profiles of CH_4 ($\mu\text{mol/L}$), N_2O (nmol/L), NO_x ($\mu\text{mol/L}$), SO_4^{2-} ($\mu\text{mol/L}$), HS^- ($\mu\text{mol/L}$), particulate Mn and Fe ($\mu\text{mol/L}$) and dissolved Mn and Fe ($\mu\text{mol/L}$) concentrations for the six field campaigns. Horizontal dashed lines represent the anoxic layer for each season (same color code).

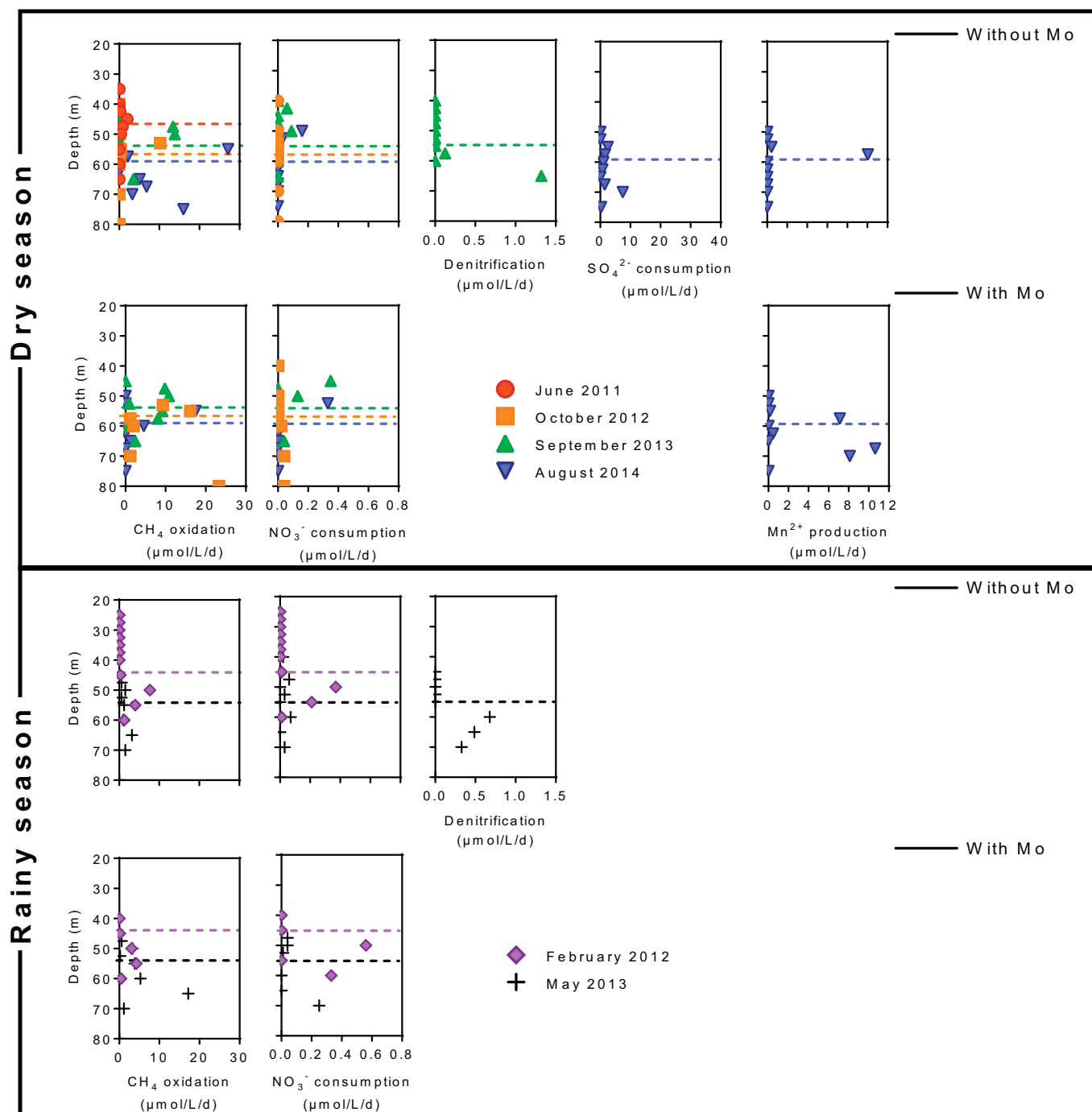


Fig. 4. Process rates (CH_4 oxidation, NO_3^- consumption, denitrification, SO_4^{2-} consumption and dissolved Mn production; $\mu\text{mol/L/d}$) without and with molybdate (Mo) added, during the six field campaigns (Upper box: dry season; Bottom box: rainy season). Horizontal dashed lines represent the anoxic layer for each season (same color code).

rates were 2.00 ± 0.04 and 13.9 ± 0.0 $\mu\text{mol/L/d}$, while maximum anoxic rates were 0.80 ± 0.01 (at 47.5 m) and 3.50 ± 0.30 (at 65 m) $\mu\text{mol/L/d}$, in June 2011 and September 2013, respectively. In October 2012, the CH_4 oxidation rate ($0.20 \mu\text{mol/L/d}$) observed in anoxic waters was negligible compared with the high rate of $10.20 \pm 0.40 \mu\text{mol/L/d}$ observed in oxic waters. NO_3^- consumption rates (ESM Table S4) tended to be low during all campaigns, but a non-negligible denitrification rate of $1.5 \mu\text{mol NO}_3^-/\text{L/d}$ was observed at 65 m in September 2013, in parallel incubations. Depth-integrated CH_4 oxidation rates were $9 \text{ mmol/m}^2/\text{d}$ in June 2011, $27 \text{ mmol/m}^2/\text{d}$ in October 2012, $81 \text{ mmol/m}^2/\text{d}$ in September 2013, and $162 \text{ mmol/m}^2/\text{d}$ in August 2014. The fraction of CH_4

oxidized in anaerobic waters was variable during dry season, ranging between 1% (October 2012) and 55% (August 2014) (Table 1)

During the rainy season, maximum CH_4 oxidation rates in anoxic waters were higher than in oxic waters. In February 2012, the maximum anoxic CH_4 oxidation rate of $7.7 \pm 0.4 \mu\text{mol/L/d}$ was observed at 50 m and co-occurred with the maximum NO_3^- consumption rate of $0.4 \pm 0.1 \mu\text{mol/L/d}$. In May 2013, the maximum anoxic CH_4 oxidation rate of $3.2 \mu\text{mol/L/d}$ was observed at 65 m, which was in the vicinity of a NO_3^- consumption rate of $0.03 \pm 0.01 \mu\text{mol/L/d}$ observed at 70 m depth (ESM Table S4). Also, higher rates of denitrification (based on ^{15}N) were observed between 60 and 70 m depth, with a maximum of

Table 1

Depth-integrated CH_4 oxidation rates ($\text{mmol/m}^2/\text{d}$) in Lake Kivu and the percent related to anaerobic oxidation of methane (AOM).

	Integration depth interval (m)	CH_4 oxidation ($\text{mmol/m}^2/\text{d}$)	% AOM
Dry season			
June 2011	1–65	9	30
October 2012	1–80	27	1
September 2013	1–65	81	15
August 2014	1–75	162	55
Rainy season			
February 2012	1–60	63	99
May 2013	1–80	44	81

$0.7 \mu\text{mol NO}_3^-/\text{L}/\text{d}$ at 60 m depth. No oxic CH_4 oxidation was observed in February 2012, while a maximum rate of $1.5 \pm 0.2 \mu\text{mol/L}/\text{d}$ was observed in May 2013. Depth-integrated CH_4 oxidation rates were $63 \text{ mmol/m}^2/\text{d}$ in February 2012 and $44 \text{ mmol/m}^2/\text{d}$ in May 2013. The fraction of CH_4 oxidized in anaerobic waters was higher and less variable during rainy season: 99% in February 2012 and 81% in May 2013 (Table 1).

Overall, CH_4 oxidation rates in oxic waters were very high when considered in the context of the initial CH_4 concentrations and relative to rates in anoxic waters (ESM Table S2). For example, the maximum CH_4 oxidation rate of $27 \pm 2 \mu\text{mol/L}/\text{d}$ observed at 55 m depth in August 2014 occurred at CH_4 concentrations of $42 \pm 2 \mu\text{mol/L}$. But this rate applied over a period of 24 h, and 68% of the initial CH_4 was consumed after 24 h. The same observation can be made, for example, in June 2011 (at 42.5 and 45 m), February 2012 (at 50 m) and October 2012 (at 53 m).

Responses to molybdate inhibitor additions were variable. In February 2012 and August 2014, CH_4 oxidation rates decreased when molybdate was added, while rates tended to increase when molybdate was added during the other field campaigns. In October 2012 and May 2013 in particular, CH_4 oxidation rates strongly increased when molybdate was added, from zero without molybdate to $23.0 \pm 0.4 \mu\text{mol/L}/\text{d}$ with molybdate (at 80 m) and from $3 \mu\text{mol/L}/\text{d}$ without molybdate to $17 \mu\text{mol/L}/\text{d}$ with molybdate (at 65 m), respectively. In September 2013, CH_4 oxidation rates increased when molybdate was added up to $9.0 \pm 0.5 \mu\text{mol/L}/\text{d}$ at 55 m. In August 2014, the addition of molybdate was also mirrored by a strong increase of dissolved Mn (Mn^{2+}) production rates. NO_3^- consumption rates also tended to increase when molybdate was added during all field campaigns (ESM Table S2). No dissolved Fe (Fe^{2+}) production was observed with or without molybdate added (data not shown).

CH_4 production was observed during the three sampled campaigns, with rates up to $0.37 \mu\text{mol/L}/\text{d}$ in August 2014 (Fig. 5). For the three campaigns, the highest CH_4 production occurred at the base of the water mass containing relatively high chlorophyll *a* contents, just above the oxic-anoxic interface.

Discussion

Aerobic and anaerobic CH_4 oxidation in the water column of Lake Kivu

The primary aim of this study was to determine rates of CH_4 oxidation in the water column of Lake Kivu. We thus report that CH_4 oxidation occurred in both oxic and anoxic waters, with maximum rates of 27 ± 2 and $16 \pm 8 \mu\text{mol/L}/\text{d}$, respectively. We observed strong variability in CH_4 oxidation rates between our field campaigns. In June 2011, October 2012 and September 2013 (dry season), the main CH_4 oxidation pathway was aerobic, whereas in both February 2012 and May 2013 (rainy season) it was anaerobic (Table 1). In August 2014, aerobic and anaerobic oxidation rates were almost equivalent. As shown by Fig. 6, aerobic oxidation rates tended to depend on the oxygenated layer depth. Aerobic CH_4 oxidation rates tended to be higher when the

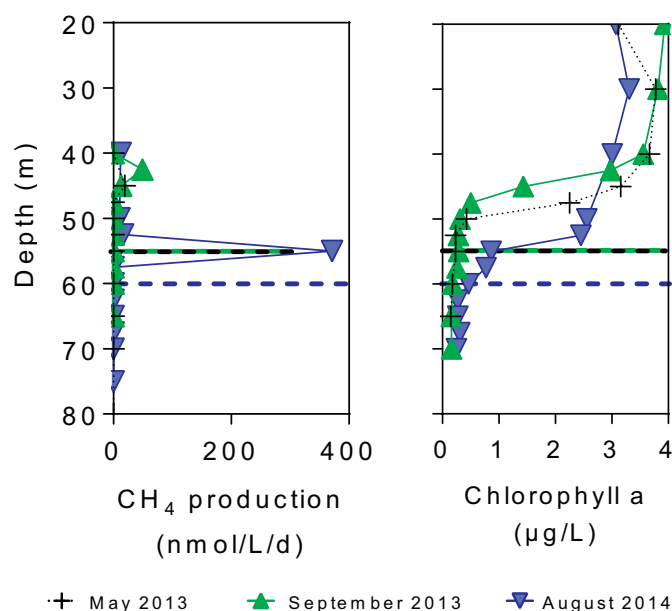


Fig. 5. Vertical profiles of CH_4 production ($\text{nmol/L}/\text{d}$) and chlorophyll *a* concentration ($\mu\text{g/L}$) in May 2013 (cross +), September 2013 (triangle Δ) and August 2014 (inverted triangle ∇). The horizontal dashed lines represent the anoxic layer for each season (same color code).

mixed layer was deeper, as usually observed during the dry season. At this time year, the oxic-anoxic interface was located closer to the chemocline, below which the CH_4 concentrations are typically 5 orders of magnitude larger than in the upper part of the mixolimnion. This observation confirms the hypothesis of Roland et al. (2016) who suggested, based on the seasonal change with depth of CH_4 concentrations, that during the dry season the depth integrated aerobic CH_4 oxidation rate was higher. On the contrary, during the rainy season, when the thermal stratification within the mixolimnion is well established, the volume of the oxic compartment is smaller than the volume of the anoxic compartment. Hence, CH_4 can only reach the oxic waters by diffusion, after that a significant fraction of the CH_4 upward flux has been oxidized by AOM, which limit the aerobic CH_4 oxidation. While

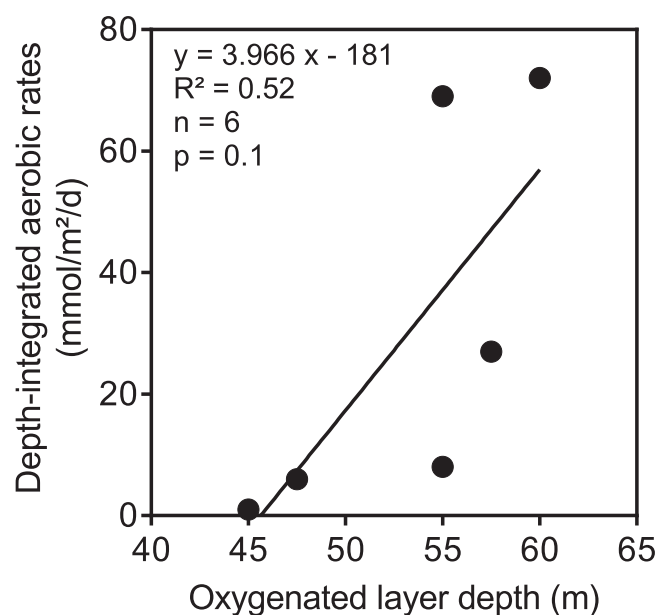


Fig. 6. Depth-integrated aerobic CH_4 oxidation rates ($\text{mmol/m}^2/\text{d}$) compared to the oxygenated layer depth (m), for all field campaigns.

Table 2Aerobic and anaerobic CH₄ oxidation rates (μmol/L/d) in Lake Kivu and other meromictic lakes in literature.

Lake	Aerobic CH ₄ oxidation (μmol/L/d) (CH ₄ concentrations; μmol/L)	AOM (μmol/L/d) (CH ₄ concentrations; μmol/L)	Source
Kivu (East Africa)	0.02–27 (0.2–42)	0.2–16 (65–689)	This study
Kivu (East Africa)	0.62 (3.6)	1.1 (54)	Pasche et al. (2011)
Pavin (France)	0.006–0.046 (0.06–0.35)	0.4 (285–785)	Lopes et al. (2011)
Big Soda (US)	0.0013 (0.1)	0.060 (50)	Iversen et al. (1987)
Marn (Sweden)	0.8 (10)	2.2 (55)	Bastviken et al. (2002)
Tanganyika (East Africa)	0.1–0.96 (<10)	0.24–1.8 (~10)	Rudd (1980)
Matano (Indonesia)	0.00036–0.0025 (0.5)	4.2–117 (12–484)	Sturm et al. (2016)

aerobic CH₄ oxidation is most probably limited by CH₄ concentrations, AOM is most probably limited by the availability of electron acceptors due to competition with more favorable processes (such as heterotrophic denitrification, sulfate reduction, etc.). Furthermore, episodic fluctuations in water column properties influence bacterial community composition and small variations in the water column structure may influence the abundance, distribution, and activity of these communities, and thus contribute to the differences observed. Nevertheless, the relatively high aerobic and anaerobic CH₄ oxidation rates measured during this study and estimated from stable isotope labelling experiments by Morana et al. (2015a) explain the low air–water CH₄ fluxes observed throughout the year in Lake Kivu (Borges et al., 2011; Roland et al., 2016).

Aerobic and anaerobic CH₄ oxidation rates are also high compared with other meromictic lakes (Table 2). The large differences observed may be explained by some characteristics of these different environments, such as the vertical structure of the water column, CH₄ concentrations, O₂ and other electron acceptor concentrations, or water temperature. Lake Kivu is a tropical lake, where the year-round high water temperatures may enhance bacterial activity in comparison with temperate and boreal lakes. Also, the strong density gradients in Lake Kivu restricts vertical mixing and promotes the accumulation of high CH₄ concentrations in anoxic waters, which slowly diffuse to the oxic compartment, supporting both aerobic and anaerobic CH₄ oxidation. The higher rates observed in Lake Matano than in Lake Kivu may be explained by higher CH₄ concentrations in anoxic waters (up to 480 μmol/L) and greater concentrations of the highly favorable electron acceptor Fe concentrations (up to 170 nmol/L) in the upper anoxic waters (Sturm et al., 2016). Also, vertical mixing in Lake Matano is stronger than in Lake Kivu (Crowe et al., 2008). Pasche et al. (2011) reported lower aerobic and anaerobic CH₄ oxidation rates in Lake Kivu than those we measured, but their CH₄ oxidation measurements were only made during one field campaign, and as we demonstrated here seasonal variability in CH₄ oxidation rates is considerable and may account for the differences observed.

Energy sources of anaerobic CH₄ oxidation in the water column of Lake Kivu

Given the theoretical stoichiometry of AOM (ESM Table S3), the vertical fluxes of electron acceptors estimated in the main basin of Lake Kivu were insufficient to sustain the integrated AOM rates. Indeed, the vertical downward SO₄^{2−} flux (average 0.3 mmol/m²/d) could have sustained 0.2–3.3% of the measured AOM. Similarly, fluxes of NO₃[−] (0.2–2.8%) Mn (<0.1%) and Fe (0.1%) oxides could only have sustained a minor fraction of AOM, even considering an extreme scenario in which the entire upward flux of NH₄⁺, Mn²⁺ and Fe²⁺ would be oxidized and the resulting electron acceptors directly available to AOM. Reports of imbalance between fluxes of potential oxidant/reductant and processes measurements in permanently stratified water bodies are common in literature (Murray et al., 1995; Taylor et al., 2001; Li et al., 2012). In Lake Kivu, Morana et al. (2016) also found significantly larger chemoautotrophic rates than could be sustained by potential fluxes of electron donors. This apparent discrepancy between the biological demand and the physical supply of electron acceptors would imply that intensive, yet cryptic, recycling of substrates occurred in the chemocline

of Lake Kivu, as also suggested in the Cariaco Basin (Li et al., 2012). Furthermore, the seasonal density gradient in the mixed layer is always weak in Lake Kivu, so that the thermal stratification that may develop within the mixolimnion, above the chemocline, is usually unstable. Episodic intrusions of SO₄^{2−}, or NO₃[−], down to the chemocline could therefore contribute to sustain the methanotrophic activity.

In February 2012, the maximum rates of AOM co-occurred with the maximum rates of NO₃[−] consumption (Fig. 4) suggesting that a fraction of the AOM measured might have been coupled to NO₃[−] reduction. NO₃[−] consumption rates are not unique indicators of denitrification in our experiments, because the NO₃[−] consumption recorded might reflect incorporation of N into biomass, or reduction to ammonium. However, significant denitrification rates were measured in a parallel experiment carried out in the Northern Basin in 2011 and 2012 at depths close to those where we observed high rates of AOM (Roland et al., 2017). In May and September 2013, we also detected denitrification activity in parallel incubations, with higher rates of denitrification corresponding to higher rates of AOM. Potential rates of AOM calculated based on the NO₃[−] consumption rates measured in the incubations and on the rates of denitrification measured in parallel incubations (Fig. 7B), according to the stoichiometric equation B (ESM Table S3), are shown in Fig. 7A and 7B, respectively. In all cases, measured rates of AOM exceed the potential rates estimated from NO₃[−] consumption rates. Likewise, denitrification rates appear also insufficient to fully sustain the rates of AOM observed. This observation generally suggests that NO₃[−] may not be an important electron acceptor for AOM in Lake Kivu.

In contrast to N, the biogeochemical cycling of Fe in the water column of Lake Kivu may not be very active, because dissolved Fe could not be detected although particulate Fe concentrations were up to 15 μmol/L (Fig. 3), suggesting that Fe(II) was not actively produced and that Fe(III) reduction may not be active. Moreover, in August 2014, no Fe²⁺ production was observed in the incubations we carried out, with-out and with molybdate added, which would tend to support a lack of Fe reduction in the water column of Lake Kivu. It is possible, however, that detection of dissolved Fe may have been eluded during our analyses given the rapid oxidation kinetics of Fe(II) with O₂, and the high potential for exposure to O₂ during our sampling and filtration. At the same time, FeS has a relatively low solubility, and formation of FeS in the presence of sulfide would tend to limit dissolved Fe concentrations (Crowe et al., 2008). Particulate and dissolved Fe fluxes could explain <1% of the integrated AOM rates for all campaigns, according to the stoichiometric Eq. C (ESM Table S3). Thus, while our experiments imply that Fe does not play a significant role in AOM, more detailed experiments would be required to conclusively rule out Fe cycling in Lake Kivu's water column.

Particulate Mn and Mn²⁺ concentrations were also measured in May 2013, September 2013 and August 2014 (Fig. 3). Particulate Mn concentrations were very low compared to dissolved Mn concentrations, with a peak located just above the oxic–anoxic interface, for each campaign. Jones et al. (2011) observed a similar profile in Lake Matano, and proposed that Mn is recycled at least 15 times across the oxic–anoxic boundary before sedimenting. Mn²⁺ is probably oxidized in presence of small quantities of O₂, precipitates and is directly reduced in anoxic waters. The same processes might occur in Lake Kivu, and MnO₂ might thus contribute to AOM at depths close to the oxic–anoxic

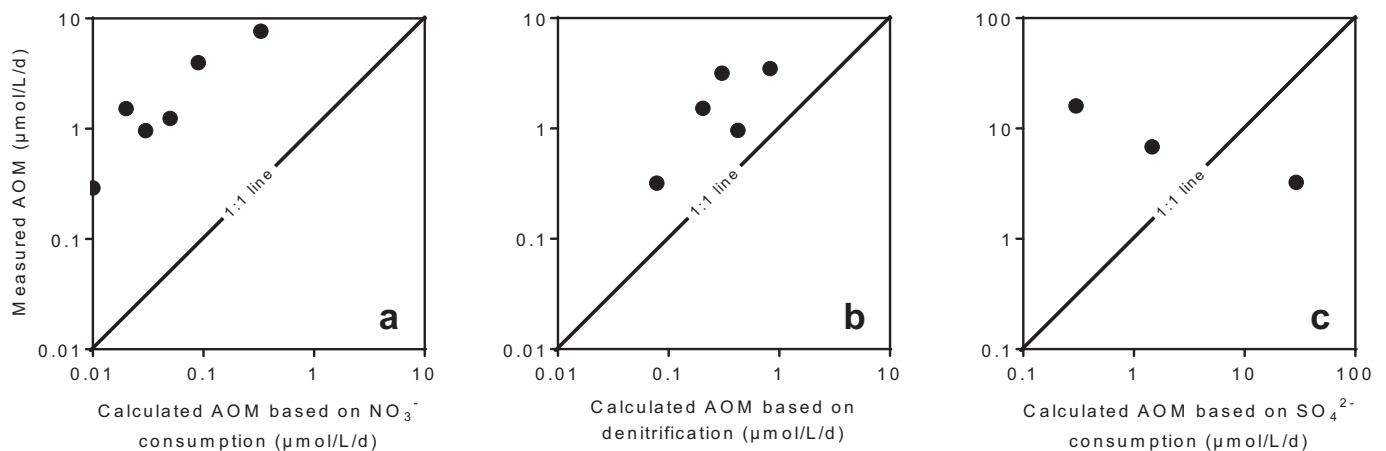


Fig. 7. Comparison between measured and calculated AOM rates ($\mu\text{mol/L/d}$) based on (A) NO_3^- consumption rates, (B) denitrification and (C) SO_4^{2-} consumption rates, for all field campaigns. Note the log scales.

interface. However, particulate Mn and Mn^{2+} fluxes were very low and could only explain <1% of the AOM rates observed. Moreover, these fluxes invoke two conditions: 1) that all the Mn^{2+} measured at each depth results from the reduction of MnO_2 , and 2) that all the Mn^{2+} measured results from MnO_2 reduction with CH_4 . Both of these conditions are unlikely, since Mn^{2+} present at these depths also originates from diffusion from below, and MnO_2 can be reduced by other electron donors than CH_4 . Also, for SO_4^{2-} and NO_x , other processes such as SO_4^{2-} reduction with organic matter and heterotrophic denitrification can take place. The percentages of AOM potentially supported by a given electron donor that are reported here are thus maximum percentages and rates. Conversely, CH_4 has the potential to be the major electron donor in the anoxic waters of Lake Kivu given the enormous amount of CH_4 dissolved in the deep waters of the lake. Indeed, the CH_4 concentration at 70 m is $\sim 385 \mu\text{mol/L}$ which is higher than the typical dissolved organic carbon concentrations of $142 \mu\text{mol/L}$ (Morana et al., 2015b). CH_4 concentrations at 70 m are also higher than the particulate organic carbon (POC) concentrations in anoxic waters, which are typically lower than $30 \mu\text{mol/L}$ (Morana et al., 2015b). In terms of carbon supply rates, the vertical CH_4 flux of $9.4 \text{ mmol/m}^2/\text{d}$ (Morana et al., 2015a) is also higher than the sedimentation flux of POC from the mixed layer of $5.2 \pm 1.7 \text{ mmol/m}^2/\text{d}$ (average value of 24-month deployment of sediment traps in the Northern Basin from November 2012 to November 2014, unpublished data). This is in general agreement with the high methanotrophic production in Lake Kivu ($8.2\text{--}28.6 \text{ mmol/m}^2/\text{d}$) previously estimated by Morana et al. (2015a).

Sulfate-dependent anaerobic CH_4 oxidation and effects of the molybdate inhibitor in the sulfate-reducing bacterial activity

Moderate SO_4^{2-} concentrations were observed in the water column of Lake Kivu (Fig. 3). Due to these higher concentrations compared with other potential electron acceptors (mean of 103, 0.40, 0.42 and $4.9 \mu\text{mol/L}$ for SO_4^{2-} , NO_x , particulate Mn and particulate Fe, respectively, at depths where AOM was observed), we hypothesized that AOM in Lake Kivu is mainly coupled to SO_4^{2-} reduction. However, the addition of the inhibitor of SRB activity (molybdate) did not allow us to clearly demonstrate SO_4^{2-} -dependent AOM. Indeed, the response of AOM to molybdate addition was variable, and about half of the measurements gave lower rates with molybdate added (suggesting the occurrence of AOM coupled to SO_4^{2-} reduction), and the other half gave higher rates (ESM Fig. S1). Measurements of SO_4^{2-} consumption rates performed in August 2014 showed that SO_4^{2-} consumption could be high enough to occasionally sustain AOM (Fig. 7C) (Equation E, ESM Table S3).

While CH_4 oxidation rates were lower in February 2012 and August 2014 when the molybdate inhibitor was added, they were higher in May and September 2013. We first considered if we inadvertently induced aerobic oxidation by injecting oxygen along with the molybdate solution, but the addition of O_2 could only have increased the oxidation rates by 6.8% (median). Even if artificially enhanced aerobic CH_4 oxidation can be ruled out, the O_2 supply could lead to production of other oxidized species like NO_3^- or particulate Fe and Mn, and thus increase rates of AOM coupled to reduction of these electron acceptors. However, no increase in the concentrations of these species was observed during the incubations with molybdate (data not shown). Moreover, since HS^- oxidation is very fast (Canfield et al., 2005), it is very likely that the inadvertently introduced O_2 was directly consumed through HS^- oxidation. The variation of the free Gibbs energy (ΔG°) is shown in ESM Table S5 for the oxidation of the different reduced elements, calculated according to Eq. 6 (Libes, 1992):

$$\Delta G^\circ = 2.303 nRT (\text{pe}_2^0 - \text{pe}_1^0) \quad (6)$$

where n is the number of electron transferred, R is the gas constant (J/mol/K), T is the absolute temperature (K), pe_1^0 and pe_2^0 are the electron activity for both reactions at constant temperature (25°C) and pH (7). It shows that the oxidation of H_2S is the most favorable process from a purely thermodynamic point of view, and thus that microorganisms can obtain larger amounts of energy by oxidizing H_2S than the other elements. This tends to support that the small amounts of O_2 artificially supplied with the addition of molybdate were probably consumed by H_2S oxidation in SO_4^{2-} . It is thus likely that SO_4^{2-} concentrations in the incubations with molybdate were higher (with no influence on AOM rates, since molybdate inhibits SO_4^{2-} reduction).

We thus hypothesize that a modification in competitive relationships between bacterial community members in presence of molybdate, such as a decrease in competition between denitrifying bacteria and/or Mn-reducing bacteria and SRB for otherwise limiting nutrients and substrates, could explain the higher NO_3^- consumption rates observed with molybdate added. Also, Mn^{2+} production rates increased with molybdate in August 2014. Competitive relationships for electron donors among members of bacterial communities have been reported in the literature (e.g. Westermann and Ahring, 1987; Achnich et al., 1995). In Lake Kivu, it is unlikely that the strong increase in AOM rates was only due to a change in competition between SRB and denitrifying bacteria and/or SRB and Mn-reducing bacteria, since NO_3^- and MnO_2 concentrations are otherwise insufficiently abundant to account for the rates of AOM observed. Another explanation may be that molybdate inhibits the activity of facultative bacteria that canonically conduct SO_4^{2-} reduction, rather than SO_4^{2-} reduction itself. It has been shown that

canonically SRB can also derive their energy via others biochemical pathways, such as denitrification, iron reduction, etc. (e.g.: *Dalsgaard and Bak, 1994*). The inhibition of such bacteria by molybdate could thus influence the balance between these different biogeochemical processes. A third explanation could be that the addition of the oxic molybdate solution supplies small quantities of oxygen (maximum 1.25 $\mu\text{mol/L}$), leading to the inhibition of strict anaerobic microorganisms growth and thus to strong modifications in the viability of specific microbial community members. With the present dataset, however, we are unable to discriminate between these possible scenarios, and further studies are required to determine the specific effects of molybdate amendments on bacterial community metabolism and interactions. To this end, it would be informative to determine how bacterial community composition is affected by the molybdate amendment.

Aerobic methanogenesis in the water column of Lake Kivu

Aerobic CH_4 oxidation in Lake Kivu is probably mainly limited by CH_4 concentrations. Indeed, CH_4 concentrations are highest in the anoxic deep waters, where it has been assumed to be exclusively produced through acetoclastic and hydrogenotrophic methanogenesis (*Pasche et al., 2011*). However, we show here that part of CH_4 present in oxic waters is likely produced through aerobic CH_4 production. During our study, the aerobic CH_4 production peaks were always located at the base of the waters containing high chlorophyll *a* concentrations. This may be due to a spatial overlap between the presence of substrates produced by phytoplankton and oxygen tolerant methanogenic archaea, as suggested by the studies of *Grossart et al. (2011)*, *Bogard et al. (2014)*, *Tang et al. (2014)* and *Tang et al. (2016)*. Indeed, *Inceoglu et al. (2015)* revealed the presence of methanogenic archaea in the anoxic waters and at the oxic-anoxic interface in Lake Kivu, including the *Methanosarcinales*. *Angel et al. (2011)* showed that some archaea belonging to *Methanosarcinales* are capable of methanogenesis under oxic conditions, in soils microcosms, albeit at lower rates than under anoxic conditions.

Conclusions

We described and quantified several processes involved in the CH_4 cycling in Lake Kivu, documenting the occurrence of AOM and aerobic CH_4 production as well as their seasonal variability. We were not able to definitively identify the main electron acceptor for AOM; however, the imbalance between CH_4 oxidation rates and vertical substrate fluxes would imply that a substantial amount of inorganic molecules is recycled in the deeper part of the mixolimnion. A seasonal variability in the respective importance of aerobic and anaerobic CH_4 oxidation rates was observed, with greater importance of aerobic oxidation in dry season and AOM in rainy season. Overall, our study demonstrates that both aerobic and anaerobic CH_4 oxidation are important for regulating CH_4 efflux from Lake Kivu. We also suggest that aerobic CH_4 production may play an important role in CH_4 cycling in Lake Kivu's mixolimnion and can contribute to Lake Kivu's CH_4 budgets. Improvements in quantifying Lake Kivu's CH_4 cycle and budgets could come from more knowledge on the electron acceptors that support AOM and the regulation and rates of aerobic CH_4 production, and such knowledge would go a long way towards knowing how CH_4 cycling works in freshwaters more generally and lead to better predictions of CH_4 effluxes from lakes in light of global change. To our best knowledge, this is the first study to report such a diversified CH_4 cycle in a tropical great lake, in particular with regards to the occurrence of aerobic CH_4 production that is still poorly investigated in freshwater environments.

Acknowledgements

We thank the Rwanda Energy Company for the access to their platform for the sampling, Renzo Biondo (University of Liège), Laura

Bristow, Dina Holmgaard Skov and Heidi Grøn Jensen (University of Southern Denmark/Lark) for help in measurements, and an anonymous reviewer for comments that helped improving the manuscript. This study was funded by the Belgian Federal Science Policy Office (BELSPO, Belgium) under the EAGLES (East African Great lake Ecosystem Sensitivity to Changes, SD/AR/02A) project, by the Fonds National de la Recherche Scientifique (FNRS) under the MICKI (Microbial diversity and processes in Lake Kivu, 1715859) project, and contributes to the European Research Council (ERC) starting grant project AFRIVAL (African river basins: Catchment-scale carbon fluxes and transformations, 240002). GC was acquired with funds from the FNRS (contract no. 2.4.598.07). AVB is a senior research associate at the FNRS. FAER had a PhD grant from FNRS («Fonds pour la formation à la Recherche dans l'Industrie et dans l'Agriculture» - FRIA).

Appendix A. Supplementary data

Supplementary data to this article can be found online at <https://doi.org/10.1016/j.jglr.2018.04.003>.

References

- Å Norðri, K., Thamdrup, B., 2014. Nitrate-dependent anaerobic methane oxidation in a freshwater sediment. *Geochim. Cosmochim. Acta* 132, 141–150.
- Å Norðri, K., Thamdrup, B., Schubert, C.J., 2013. Anaerobic oxidation of methane in an iron-rich Danish freshwater lake sediment. *Limnol. Oceanogr.* 58, 546–554.
- Achnich, C., Bak, F., Conrad, R., 1995. Competition for electron donors among nitrate reducers, ferric iron reducers, sulfate reducers, and methanogens in anoxic paddy soil. *Biol. Fertil. Soils* 19, 65–72.
- Angel, R., Matthies, D., Conrad, R., 2011. Activation of methanogenesis in arid biological soil crusts despite the presence of oxygen. *PLoS One* 6, e20453.
- APHA, 1998. *Standard Methods for the Examination of Water and Wastewater*. American Public Health Association.
- Bastviken, D., Ejlertsson, J., Tranvik, L., 2002. Measurement of methane oxidation in lakes: a comparison of methods. *Environ. Sci. Technol.* 36, 3354–3361.
- Bastviken, D., Tranvik, L.J., Downing, J.A., Crill, P.M., Enrich-Prast, A., 2011. Freshwater methane emissions offset the continental carbon sink. *Science* 331, 50.
- Beal, E.J., House, C.H., Orphan, V.J., 2009. Manganese- and iron-dependent marine methane oxidation. *Science* 325, 184–187.
- Boetius, A., Ravensschlag, K., Schubert, C.J., Rickert, D., Widdel, F., Gieseke, A., Amann, R., Jørgensen, B.B., Witte, U., Pfannkuche, O., 2000. A marine microbial consortium apparently mediating anaerobic oxidation of methane. *Nature* 407, 623–626.
- Bogard, M.J., del Giorgio, P.A., Boutet, L., Chaves, M.C.G., Prairie, Y.T., Merante, A., Derry, A.M., 2014. Oxic water column methanogenesis as a major component of aquatic CH_4 fluxes. *Nat. Commun.* 5.
- Borges, A.V., Abril, G., Delille, B., Descy, J.P., Darchambeau, F., 2011. Diffusive methane emissions to the atmosphere from Lake Kivu (Eastern Africa). *J. Geophys. Res. Biogeosci.* 116.
- Borges, A.V., Darchambeau, F., Teodoru, C.R., Marwick, T.R., Tamooh, F., Geeraert, N., Omengo, F.O., Guérin, F., Lambert, T., Morana, C., 2015. Globally significant greenhouse-gas emissions from African inland waters. *Nat. Geosci.* 8, 637–642.
- Borrel, G., Jézéquel, D., Biderre-Petit, C., Morel-Desrosiers, N., Morel, J.-P., Peyret, P., Fonty, G., Lehours, A.-C., 2011. Production and consumption of methane in freshwater lake ecosystems. *Res. Microbiol.* 162, 832–847.
- Braman, R.S., Hendrix, S.A., 1989. Nitrone nitrite and nitrate determination in environmental and biological materials by vanadium(III) reduction with chemiluminescence detection. *Anal. Chem.* 61, 2715–2718.
- Canfield, D.E., Kristensen, E., Thamdrup, B., 2005. The sulfur cycle. *Adv. Mar. Biol.* 48, 313–381.
- Cline, J.D., 1969. Spectrophotometric determination of hydrogen sulfide in natural waters. *Limnol. Oceanogr.* 14, 454–458.
- Conrad, R., 2009. The global methane cycle: recent advances in understanding the microbial processes involved. *Environ. Microbiol. Rep.* 1, 285–292.
- Crowe, S.A., O'Neill, A.H., Katsev, S., Hehanussa, P., Haffner, G.D., Sundby, B., Mucci, A., Fowle, D.A., 2008. The biogeochemistry of tropical lakes: a case study from Lake Matano, Indonesia. *Limnol. Oceanogr.* 53, 319–331.
- Crowe, S., Katsev, S., Leslie, K., Sturm, A., Magen, C., Nomosatryo, S., Pack, M., Kessler, J., Reeburgh, W., Roberts, J., 2011. The methane cycle in ferruginous Lake Matano. *Geobiology* 9, 61–78.
- Cui, M., Ma, A., Qi, H., Zhuang, X., Zhuang, G., 2015. Anaerobic oxidation of methane: an “active” microbial process. *Microbiology* 4, 1–11.
- Dalsgaard, T., Bak, F., 1994. Nitrate reduction in a sulfate-reducing bacterium, *Desulfovibrio desulfuricans*, isolated from rice paddy soil: sulfide inhibition, kinetics, and regulation. *Appl. Environ. Microbiol.* 60, 291–297.
- Deutzmann, J.S., Schink, B., 2011. Anaerobic oxidation of methane in sediments of Lake Constance, an oligotrophic freshwater lake. *Appl. Environ. Microbiol.* 77, 4429–4436.
- Ettwig, K.F., Butler, M.K., Le Paslier, D., Pelletier, E., Mangenot, S., Kuypers, M.M., Schreiber, F., Dutilleul, B.E., Zedelius, J., De Beer, D., 2010. Nitrite-driven anaerobic methane oxidation by oxygenic bacteria. *Nature* 464, 543–548.

- Ettwig, K.F., Zhu, B., Speth, D., Keltjens, J.T., Jetten, M.S.M., Kartal, B., 2016. Archaea catalyze iron-dependent anaerobic oxidation of methane. *PNAS* 113, 12792–12796.
- Grossart, H.-P., Frindte, K., Dzialis, C., Eckert, W., Tang, K.W., 2011. Microbial methane production in oxygenated water column of an oligotrophic lake. *PNAS* 108, 19657–19661.
- Haroon, M.F., Hu, S., Shi, Y., Imelfort, M., Keller, J., Hugenholtz, P., Yuan, Z., Tyson, G.W., 2013. Anaerobic oxidation of methane coupled to nitrate reduction in a novel archaeal lineage. *Nature* 500, 567–570.
- Hu, S., Zeng, R.J., Keller, J., Lant, P.A., Yuan, Z., 2011. Effect of nitrate and nitrite on the selection of microorganisms in the denitrifying anaerobic methane oxidation process. *Environ. Microbiol. Rep.* 3, 315–319.
- Hu, B.L., Shen, L.D., Lian, X., Zhu, Q., Liu, S., Huang, Q., He, Z.F., Geng, S., Cheng, D.Q., Lou, L.P., Xu, X.Y., Zheng, P., He, Y.-F., 2014. Evidence for nitrite-dependent anaerobic methane oxidation as a previously overlooked microbial methane sink in wetlands. *PNAS* 111, 4495–4500.
- Inceoglu, Ö., Lirós, M., García-Armisen, T., Crowe, S.A., Michiels, C., Darchambeau, F., Descy, J.-P., Servais, P., 2015. Distribution of bacteria and archaea in meromictic tropical Lake Kivu (Africa). *Aquat. Microb. Ecol.* 74, 215–233.
- Iversen, N., Jørgensen, B., 1985. Anaerobic methane oxidation rates at the sulfate-methane transition in marine sediments from Kattegat and Skagerrak (Denmark). *Limnol. Oceanogr.* 30, 944–955.
- Iversen, N., Oremland, R.S., Klug, M.J., 1987. Big Soda Lake (Nevada). 3. Pelagic methanogenesis and anaerobic methane oxidation. *Limnol. Oceanogr.* 32, 804–814.
- Jannasch, H.W., 1975. Methane oxidation in Lake Kivu (central Africa). *Limnol. Oceanogr.* 20, 860–864.
- Jarrell, K.F., 1985. Extreme oxygen sensitivity in methanogenic Archaeobacteria. *Bioscience* 35, 298–302.
- Jones, C., Crowe, S.A., Sturm, A., Leslie, K.L., MacLean, L.C.W., Katsev, S., Henny, C., Fowle, D.A., Canfield, D.E., 2011. Biogeochemistry of manganese in ferruginous Lake Matano, Indonesia. *Biogeochemistry* 8, 2977–2991.
- Jørgensen, B.B., Weber, A., Zopfi, J., 2001. Sulfate reduction and anaerobic methane oxidation in Black Sea sediments. *Deep-Sea Res. Pt. I* 48, 2097–2120.
- Karl, D.M., Beversdorf, L., Björkman, K.M., Church, M.J., Martinez, A., Delong, E.F., 2008. Aerobic production of methane in the sea. *Nat. Geosci.* 1, 473–478.
- Kirschke, S., Bousquet, P., Ciais, P., Saunio, M., Canadell, J.G., Dlugokencky, E.J., Bergamaschi, P., Bergmann, D., Blake, D.R., Bruhwiler, L., Cameron-Smith, P., Castaldi, S., Chevallier, F., Feng, L., Fraser, A., Heimann, M., Hodson, E.L., Houweling, S., Josse, B., Fraser, P.J., Krummel, P.B., Lamarque, J.-F., Langenfelds, R.L., Le Quer, C., Naik, V., O'Doherty, S., Palmer, P.I., Pison, I., Plummer, D., Poulter, B., Prinn, R.G., Rigby, M., Ringeval, B., Santini, M., Schmidt, M., Shindell, D.T., Simpson, I.J., Spahn, R., Steele, L.P., Strode, S.A., Sudo, K., Zappa, S., van der Werf, G.R., Voulgarakis, A., van Weele, M., Weiss, R.F., Williams, J.E., Zeng, G., 2013. Three decades of global methane sources and sinks. *Nat. Geosci.* 6, 813–823.
- Lenhart, K., Klintzsch, T., Langer, G., Nehrk, G., Bunge, M., Schnell, S., Keppler, F., 2016. Evidence for methane production by the marine algae *Emiliania huxleyi*. *Biogeochemistry* 13, 3163–3174.
- Li, X.N., Taylor, G.T., Astor, Y., Varela, R., Scranton, M.I., 2012. The conundrum between chemoautotrophic production and reductant and oxidant supply: a case study from the Cariaco Basin. *Deep Sea Res. Part 1 Oceanogr. Res. Pap.* 61, 1–10.
- Libes, S.M., 1992. An Introduction to Marine Biogeochemistry. John Wiley & Sons.
- Lopes, F., Viollier, E., Thiam, A., Michard, G., Abril, G., Groleau, A., Prévot, F., Carrias, J.-F., Albéric, P., Jézéquel, D., 2011. Biogeochemical modelling of anaerobic vs. aerobic methane oxidation in a meromictic crater lake (Lake Pavin, France). *Appl. Geochem.* 26, 1919–1932.
- Megraw, S.R., Knowles, R., 1990. Effect of picolinic acid (2-pyridine carboxylic acid) on the oxidation of methane and ammonia in soil and in liquid culture. *Soil Biol. Biochem.* 22, 635–641.
- Miranda, K.M., Espey, M.G., Wink, D.A., 2001. A rapid, simple spectrophotometric method for simultaneous detection of nitrate and nitrite. *Nitric Oxide Biol. Chem.* 5, 62–71.
- Morana, C., Darchambeau, F., Roland, F.A.E., Borges, A.V., Muvundja, F.A., Kelemen, Z., Masilya, P., Descy, J.P., Bouillon, S., 2015a. Biogeochemistry of a large and deep tropical lake (Lake Kivu, East Africa): insights from a stable isotope study covering an annual cycle. *Biogeochemistry* 12, 4953–4963.
- Morana, C., Borges, A.V., Roland, F.A.E., Darchambeau, F., Descy, J.P., Bouillon, S., 2015b. Methanotrophy within the water column of a large meromictic tropical lake (Lake Kivu, East Africa). *Biogeochemistry* 12, 2077–2088.
- Morana, C., Roland, F.A., Crowe, S.A., Lirós, M., Borges, A.V., Darchambeau, F., Bouillon, S., 2016. Chemoautotrophy and anoxygenic photosynthesis within the water column of a large meromictic tropical lake (Lake Kivu, East Africa). *Limnol. Oceanogr.* 61, 1424–1437.
- Murray, J.W., Codispoti, L.A., Friederich, G.E., 1995. Oxidation-reduction environments. *Aquatic Chemistry. American Chemical Society*, pp. 157–176.
- Nisbet, E.G., Dlugokencky, E.J., Manning, M.R., Lowry, D., Fisher, R.E., France, J.L., Michel, S.E., Miller, J.B., White, J.W.C., Vaughn, B., Bousquet, P., Pyle, J.A., Warwick, N.J., Cain, M., Brownlow, R., Zazzeri, G., Laniosell, M., Manning, A.C., Gloor, E., Worthly, D.E.J., Brunke, E.G., Labuschagne, C., Wolff, E.W., Ganesan, A.L., 2016. Rising atmospheric methane: 2007–2014 growth and isotopic shift. *Glob. Biogeochem. Cycles* 30, 1356–1370.
- Pasche, N., Dinkel, C., Mu, B., Schmid, M., Wu, A., Wehrli, B., 2009. Physical and biogeochemical limits to internal nutrient loading of meromictic Lake Kivu. *Limnol. Oceanogr.* 54, 1863–1873.
- Pasche, N., Schmid, M., Vazquez, F., Schubert, C.J., Wüest, A., Kessler, J.D., Pack, M.A., Reeburgh, W.S., Bürgmann, H., 2011. Methane sources and sinks in Lake Kivu. *J. Geophys. Res. Biogeosci.* 116, G03006.
- Raghoebaring, A.A., Pol, A., Van de Pas-Schoonen, K.T., Smolders, A.J., Ettwig, K.F., Rijpstra, W.I.C., Schouten, S., Damsté, J.S.S., den Camp, H.J.O., Jetten, M.S., 2006. A microbial consortium couples anaerobic methane oxidation to denitrification. *Nature* 440, 918–921.
- Rodier, J., Bazin, C., Broutin, J., Chambon, P., Champsaur, H., Rodi, L., 1996. L'Analyse de l'Eau (8ème éd.). Dunod, Paris, France.
- Roland, F.A.E., Darchambeau, F., Morana, C., Borges, A.V., 2016. Nitrous oxide and methane seasonal variability in the epilimnion of a large tropical meromictic lake (Lake Kivu, East-Africa). *Aquat. Sci.* 79, 209–218.
- Roland, F.A.E., Darchambeau, F., Borges, A.V., Morana, C., De Brabandere, L., Thamdrup, B., Crowe, S.A., 2017. Denitrification, anaerobic ammonium oxidation, and dissimilatory nitrate reduction to ammonium in an east African Great Lake (Lake Kivu). *Limnol. Oceanogr.* 63, 687–701.
- Rudd, J.W., 1980. Methane oxidation in Lake Tanganyika (East Africa). *Limnol. Oceanogr.* 25, 958–963.
- Rudd, J.W.M., Hamilton, R.D., Campbell, N.E.R., 1974. Measurement of microbial oxidation of methane in lake water. *Limnol. Oceanogr.* 19, 519–524.
- Sarmiento, H., Isumbisho, M., Descy, J.-P., 2006. Phytoplankton ecology of Lake Kivu (eastern Africa). *J. Plankton Res.* 28, 815–829.
- Saunio, M., Bousquet, P., Poulter, B., Peregon, A., Ciais, P., Canadell, J.G., Dlugokencky, E.J., Etiope, G., Bastviken, D., Houweling, S., Janssens-Maenhout, G., Tubiello, F.N., Castaldi, S., Jackson, R.B., Alexe, M., Arora, V.K., Beerling, D.J., Bergamaschi, P., Blake, D.R., Brailsford, G., Brovkin, V., Bruhwiler, L., Crevoisier, C., Crill, P., Curry, C., Frankenberg, C., Gedney, N., Höglund-Isaksson, L., Ishizawa, M., Ito, A., Joos, F., Kim, H.S., Kleinen, T., Krummel, P., Lamarque, J.F., Langenfelds, R., Locatelli, R., Machida, T., Maksyutov, S., McDonald, K.C., Marshall, J., Melton, J.R., Morino, I., O'Doherty, S., Parmentier, F.J.W., Patra, P.K., Peng, C., Peng, S., Peters, G.P., Pison, I., Prigent, C., Prinn, R., Ramonet, M., Riley, W.J., Saito, M., Schroeder, R., Simpson, I.J., Spahn, R., Steele, P., Takizawa, A., Thornton, B.F., Tian, H., Tohjima, Y., Viovy, N., Voulgarakis, A., van Weele, M., van der Werf, G., Weiss, R., Wiedinmyer, C., Wilton, D.J., Wiltshire, A., Worthly, D., Wunch, D.B., Xu, X., Yoshida, Y., Zhang, B., Zhang, Z., Zhu, Q., 2016. The global methane budget: 2000–2012. *Earth Syst. Sci. Data Discuss.* 2016, 1–79.
- Schubert, C.J., Lucas, F., Durisch-Kaiser, E., Stierli, R., Diem, T., Scheidegger, O., Vazquez, F., Müller, B., 2010. Oxidation and emission of methane in a monomictic lake (Rotsee, Switzerland). *Aquat. Sci.* 72, 455–466.
- Shen, L.D., Liu, S., Zhu, Q., Li, X.Y., Cai, C., Cheng, D.Q., Lou, L.P., Xu, X.Y., Zheng, P., Hu, B.L., Shen, 2014. Distribution and diversity of nitrite-dependent anaerobic methane-oxidizing bacteria in the sediments of the Qiantang River. *Microb. Ecol.* 67, 341–349.
- Sivan, O., Adler, M., Pearson, A., Gelman, F., Bar-Or, I., John, S.G., Eckert, W., 2011. Geochemical evidence for iron-mediated anaerobic oxidation of methane. *Limnol. Oceanogr.* 56, 1536–1544.
- Sturm, A., Fowle, D.A., Jones, C., Leslie, K., Nomosatryo, S., Henny, C., Canfield, D.E., Crowe, S.A., 2016. Rates and pathways of CH₄ oxidation in ferruginous Lake Matano, Indonesia. *Biogeochemistry* 2016, 1–34.
- Tang, K.W., McGinnis, D.F., Frindte, K., Brüchert, V., Grossart, H.-P., 2014. Paradox reconsidered: methane oversaturation in well-oxygenated lake waters. *Limnol. Oceanogr.* 59, 275–284.
- Tang, K.W., McGinnis, D.F., Ionescu, D., Grossart, H.-P., 2016. Methane production in oxic lake waters potentially increases aquatic methane flux to air. *Environ. Sci. Technol. Lett.* 3, 227–233.
- Taylor, G.T., Iabichella, M., Ho, T.-Y., Scranton, M.I., Thunell, R.C., Muller-Karger, F., Varela, R., 2001. Chemoautotrophy in the redox transition zone of the Cariaco Basin: a significant midwater source of organic carbon production. *Limnol. Oceanogr.* 46, 148–163.
- Thamdrup, B., Dalsgaard, T., 2002. Production of N₂ through anaerobic ammonium oxidation coupled to nitrate reduction in marine sediments. *Appl. Environ. Microbiol.* 68, 1312–1318.
- Wang, Y., Zhu, G., Harhangi, H.R., Zhu, B., Jetten, M.S.M., Yin, C., Op den Camp, H.J.M., 2012. Co-occurrence and distribution of nitrite-dependent anaerobic ammonium and methane-oxidizing bacteria in a paddy soil. *FEMS Microbiol. Lett.* 336, 79–88.
- Weiss, R.F., 1981. Determinations of carbon dioxide and methane by dual catalyst flame ionization chromatography and nitrous oxide by electron capture chromatography. *J. Chromatogr. Sci.* 19, 611–616.
- Weiss, R.F., Price, B.A., 1980. Nitrous oxide solubility in water and seawater. *Mar. Chem.* 8, 347–359.
- Westermann, P., Ahning, B.K., 1987. Dynamics of methane production, sulfate reduction, and denitrification in a permanently waterlogged alder swamp. *Appl. Environ. Microbiol.* 53, 2554–2559.
- Yadav, V.K., Archer, D.B., 1989. Sodium molybdate inhibits sulphate reduction in the anaerobic treatment of high-sulphate molasses wastewater. *Appl. Microbiol. Biotechnol.* 31, 103–106.
- Yamamoto, S., Alcauskas, J.B., Crozier, T.E., 1976. Solubility of methane in distilled water and seawater. *J. Chem. Eng. Data* 21, 78–80.
- Zigah, P.K., Oswald, K., Brand, A., Dinkel, C., Wehrli, B., Schubert, C.J., 2015. Methane oxidation pathways and associated methanotrophic communities in the water column of a tropical lake. *Limnol. Oceanogr.* 60, 553–572.